iScience

CellPress

Article

A Strategic Target Rescues Trimethoprim Sensitivity in *Escherichia coli*

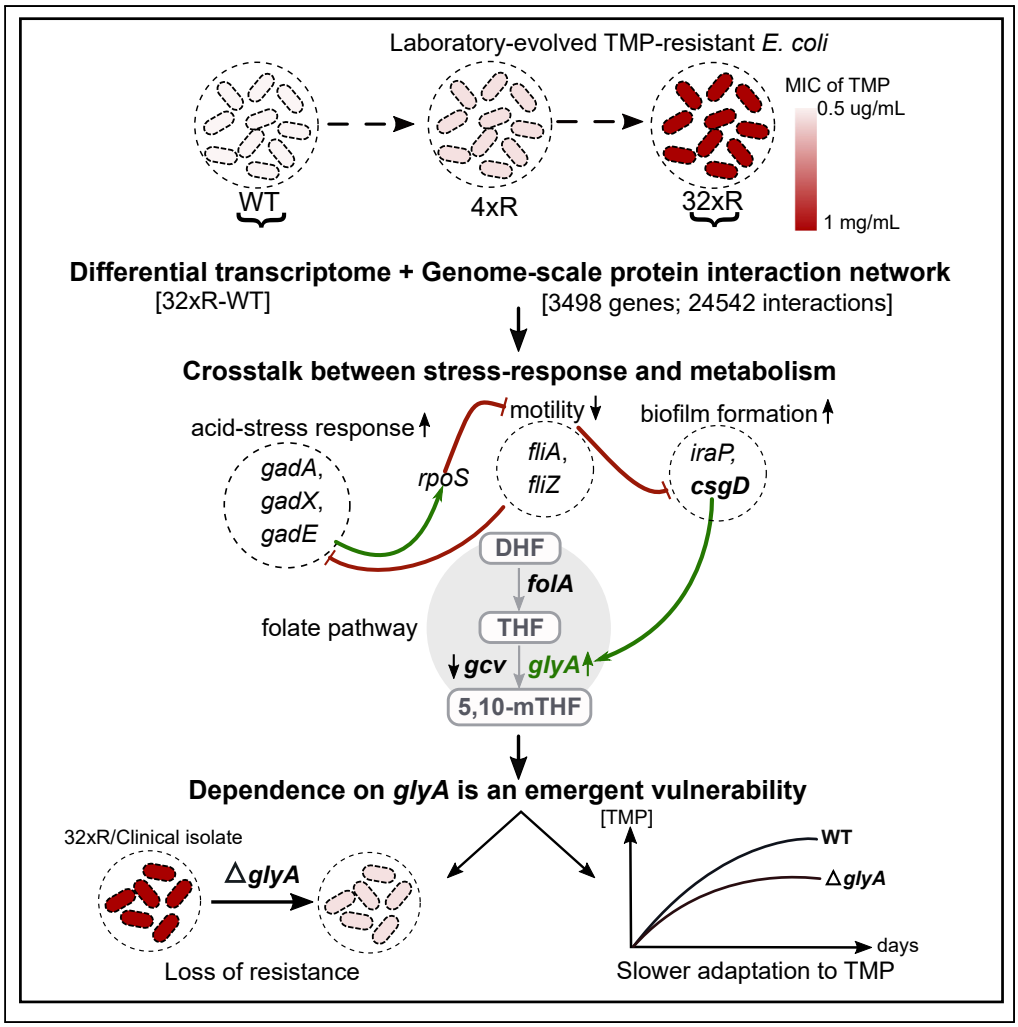

Amrisha Bhosle, Akshay Datey, Giridhar Chandrasekharan, Deepshikha Singh, Dipshikha Chakravortty, Nagasuma Chandra

dipa@iisc.ac.in (D.C.)
nchandra@iisc.ac.in (N.C.)

HIGHLIGHTS

TMP-resistant *E. coli* show cross talk between stress response and metabolic pathways

Dependence on *glyA* is an emergent vulnerability associated with TMP resistance

Knockout of *glyA* partially rescues sensitivity to TMP in *E. coli*

Bhosle et al., iScience *23*, 100986
April 24, 2020
https://doi.org/10.1016/j.isci.2020.100986

iScience

CellPress

Article

A Strategic Target Rescues Trimethoprim Sensitivity in *Escherichia coli*

Amrisha Bhosle,[1] Akshay Datey,[2] Giridhar Chandrasekharan,[3] Deepshikha Singh,[1] Dipshikha Chakravortty,[2,3,*] and Nagasuma Chandra[1,2,4,*]

SUMMARY

Trimethoprim, a preferred treatment for urinary tract infections, is becoming obsolete owing to the rapid dissemination of resistant *E. coli*. Although direct resistance mechanisms such as overexpression of a mutant FolA and *dfr* enzymes are well characterized, associated alterations that drive or sustain resistance are unknown. We identify the repertoire of resistance-associated perturbations by constructing and interrogating a transcriptome-integrated functional interactome. From the cross talk between perturbations in stress-response and metabolic pathways, we identify the critical dependence on serine hydroxymethyltransferase (GlyA) as an emergent vulnerability. Through its deletion, we demonstrate that GlyA is necessary to sustain high levels of resistance in both laboratory-evolved resistant *E. coli* and a multidrug-resistant clinical isolate. Through comparative evolution, we show that the absence of GlyA activity decelerates the acquisition of resistance in *E. coli*. Put together, our results identify GlyA as a promising target, providing a basis for the rational design of drug combinations.

INTRODUCTION

Trimethoprim (TMP) is commonly used in the treatment of urinary tract infections (UTIs) caused by *Escherichia coli* and *Klebsiella pneumoniae* (Huovinen et al., 1995). It is used either alone or in combination with sulfamethoxazole (SMX), which has a slightly different target spectrum. Although TMP and SMX are administered as a combination in the treatment of UTIs, synergy between the two has not been observed *in vivo* and, therefore, prophylaxis or treatment can be carried out using TMP alone (Acar et al., 1973; Kasanen and Sundquist, 1982). Owing to relatively low cost, it is the preferred treatment option in developing countries where incidence of UTIs is generally higher. However, in the past several decades, the use of TMP has been limited by the emergence of resistant bacteria in developed and developing countries alike (Sanchez et al., 2012; Seputiené et al., 2010).

TMP causes the depletion of deoxythymidine monophosphate (dTMP), methionine, glycine, and purines through the competitive inhibition of dihydrofolate reductase (FolA) in the folate pathway (Kwon et al., 2010). Not surprisingly, binding site mutations in FolA, which impinge on TMP binding, FolA overexpression, and acquisition of naturally resistant plasmid-borne *dfr* enzymes, are direct mechanisms of resistance in several bacteria (Flensburg and Sköld, 1987; Volpato and Pelletier, 2009; White et al., 2000). The currently explored strategies for tackling resistance include synergistic combinations and cycling of antibiotics with collateral sensitivity outcomes; although TMP in combination with SMX and vancomycin has been found to synergistically inhibit wild-type (WT) TMP-sensitive *E. coli in vitro*, some TMP-resistant *E. coli* strains have been observed to be inhibited by TMP-zidovudine (Wambaugh et al., 2017; Zhou et al., 2015). However, through drug cycling experiments it has been found that TMP-resistant *E. coli* show co-resistance to most other commonly used antibiotics, which indicates involvement of several broad-spectrum resistance mechanisms (Imamovic and Sommer, 2013). Therefore, identification of a strategic target or inhibitor through systematic investigation of the phenotype merits importance.

Transcriptomic characterization of *E. coli* upon exposure to TMP has shown that, under bacteriostatic and bactericidal conditions, expression of genes involved in the SOS response, pyrimidine synthesis and salvage, DNA repair, and *mar* operon is altered (Sangurdekar et al., 2011). Furthermore, activation of acid stress response in *E. coli* has also been observed following exposure to sub-inhibitory concentration of TMP (Mitosch et al., 2017). Several of these processes can be expected to not only be active in TMP-resistant *E. coli* but also lead to the emergence of vulnerabilities, thereby presenting new opportunities for inhibiting resistant *E. coli*. With an objective of identifying such targetable resistance-associated alterations,

[1]Department of Biochemistry, Indian Institute of Science, Bangalore, Karnataka 560012, India

[2]Center for Biosystems Science and Engineering, Indian Institute of Science, Bangalore, Karnataka 560012, India

[3]Department of Microbiology and Cell Biology, Indian Institute of Science, Bangalore, Karnataka 560012, India

[4]Lead Contact

*Correspondence: dipa@iisc.ac.in (D.C.), nchandra@iisc.ac.in (N.C.)

https://doi.org/10.1016/j.isci.2020.100986

we studied laboratory-evolved TMP-resistant *E. coli* using a transcriptome-integrated network approach. Several genes involved in stress response and metabolism were found to be differentially expressed with extensive cross talk between them. Based on the nature of metabolic perturbations, we identified the dependence on serine hydroxymethyltransferase (GlyA), an enzyme in the folate pathway as an emergent vulnerability in TMP-resistant *E. coli*. We demonstrated that the deletion of *glyA* significantly rescues sensitivity to TMP in two laboratory-evolved TMP-resistant *E. coli* strains and a multidrug-resistant (MDR) clinical isolate of uropathogenic *E. coli*. Finally, through a comparative evolution experiment, we observed that acquisition of TMP resistance is slower in the absence of *glyA*.

RESULTS AND DISCUSSION

Evolution and Transcriptome of TMP-Resistant *E. coli*

TMP-resistant *E. coli* were evolved from *E. coli* K12 MG1655 (WT) as per previous protocols (Padiadpu et al., 2016; Toprak et al., 2011). Briefly, in each step of the experiment, the concentration of TMP was doubled and *E. coli* was sub-cultured (initial A_{600} ~ 0.1) when sufficient growth (A_{600} ~ 0.6) at a particular concentration was observed. The minimum inhibitory concentration (MIC) for WT was found to be 0.5 μg/mL (consistent with the MIC expected *in vivo* with a peak serum concentration of TMP, i.e., 1–2.5 μg/mL) (Schulz and Schmoldt, 2003). Two strains—32xR1 and 32xR2—were evolved from biological replicates of WT, i.e., WT1 and WT2, respectively, starting from a sub-inhibitory concentration of 0.125–16 μg/mL (Figure 1A). Only a minor growth defect was observed for both 32xR strains in the absence and presence of 16 μg/mL TMP indicating that the resistance-associated fitness cost was minimal (Figure S1). The MIC for 32xR1 and 32xR2 was 1,024 and 128 μg/mL, respectively. Both the 32xR strains had the previously characterized Leu28Arg (L28R) TMP-resistant mutation in the binding site of FolA and the −34C>T mutation in the −35 region of the *folA* promoter, which causes an overexpression of the mutant DHFR (Mohan et al., 2015; Toprak et al., 2011). On an average, *folA* was found to be ~20-fold upregulated in the 32xR *E. coli* (Table S1). The TMP resistance of 32xR *E. coli* can be largely attributed to the presence of these mutations.

Transcriptomes of TMP-resistant (4xR1, 4xR2, 32xR1, and 32xR2) and WT *E. coli* were profiled using a DNA microarray. The 4xR *E. coli* were TMP-resistant intermediates in the evolution of 32xR *E. coli* from the WT (Figure 1A). To prevent loss of resistance, resistant *E. coli* were grown in media containing appropriate concentration of TMP; the biological replicates of WT, 4xR, and 32xR *E. coli* were grown to mid-log phase in M9, M9-2 μg/mL TMP, and M9-16 μg/mL TMP. Expression values were obtained for 4,021 genes and found to be highly correlated ($\geq$0.95) among the two biological replicates of each type of *E. coli*. Therefore, for each gene, we considered the mean of the two expression values for all analyses. Since the transcriptomes of WT *E. coli* growing in sub-inhibitory antibiotic concentrations are diverse, we compared the transcriptomes of the resistant bacteria with that of the WT grown in the absence of the drug (Erickson et al., 2017).

Totally, 397 unique differentially expressed genes (DEGs) ($|\log_2$fold-change (FC)$| \geq 1$ and Benjamini-Hochberg FDR-corrected p value < 0.05) were identified in the TMP-resistant (4xR and 32xR) *E. coli*. For the 4xR *E. coli*, 173 DEGs were identified, whereas nearly twice as many, 345, were found in the 32xR *E. coli* (Table S1). FC was observed to be higher in 32xR *E. coli* (Figure 1B). With the RNA samples used for microarray, the FC values for a few DEGs were re-estimated with qPCR and found to agree with the FC obtained from the microarray (Table S2). Between the 32xR and 4xR strains, 46 and 75 DEGs were seen to be commonly upregulated and downregulated, respectively (Figure 1C). No DEG upregulated in 4xR *E. coli* was seen to be downregulated in 32xR *E. coli* and vice versa, suggesting an absence of change in survival strategy as *E. coli* adapt to higher concentrations of TMP (Figure 1C). Adaptation to TMP was observed to occur through perturbation of several biological processes. SOS response, response to acidic pH, viral process, biofilm formation, and lipopolysaccharide metabolism were seen to be enriched in upregulated genes, whereas most of the downregulated genes were seen to be involved in chemotaxis, amino acid metabolism, pyrimidine biosynthesis, and siderophore and molybdate transport (Figure 1D). Some of these processes have also been observed in WT *E. coli* grown in sub-inhibitory TMP indicating coherence between stress response and resistance to TMP (Sangurdekar et al., 2011).

Unbiased Identification of Altered Interactions, Paths, and Cross Talk in TMP-Resistant *E. coli*

We were interested in knowing if the DEGs were functionally connected in any way. A knowledge-based functional interactome, i.e., a genome-scale protein-protein interaction network, integrated with phenotype-specific gene expression data is an elegant tool for studying underlying cross talk. Such networks have been instrumental in the identification of isoniazid resistance mechanisms in mycobacteria and

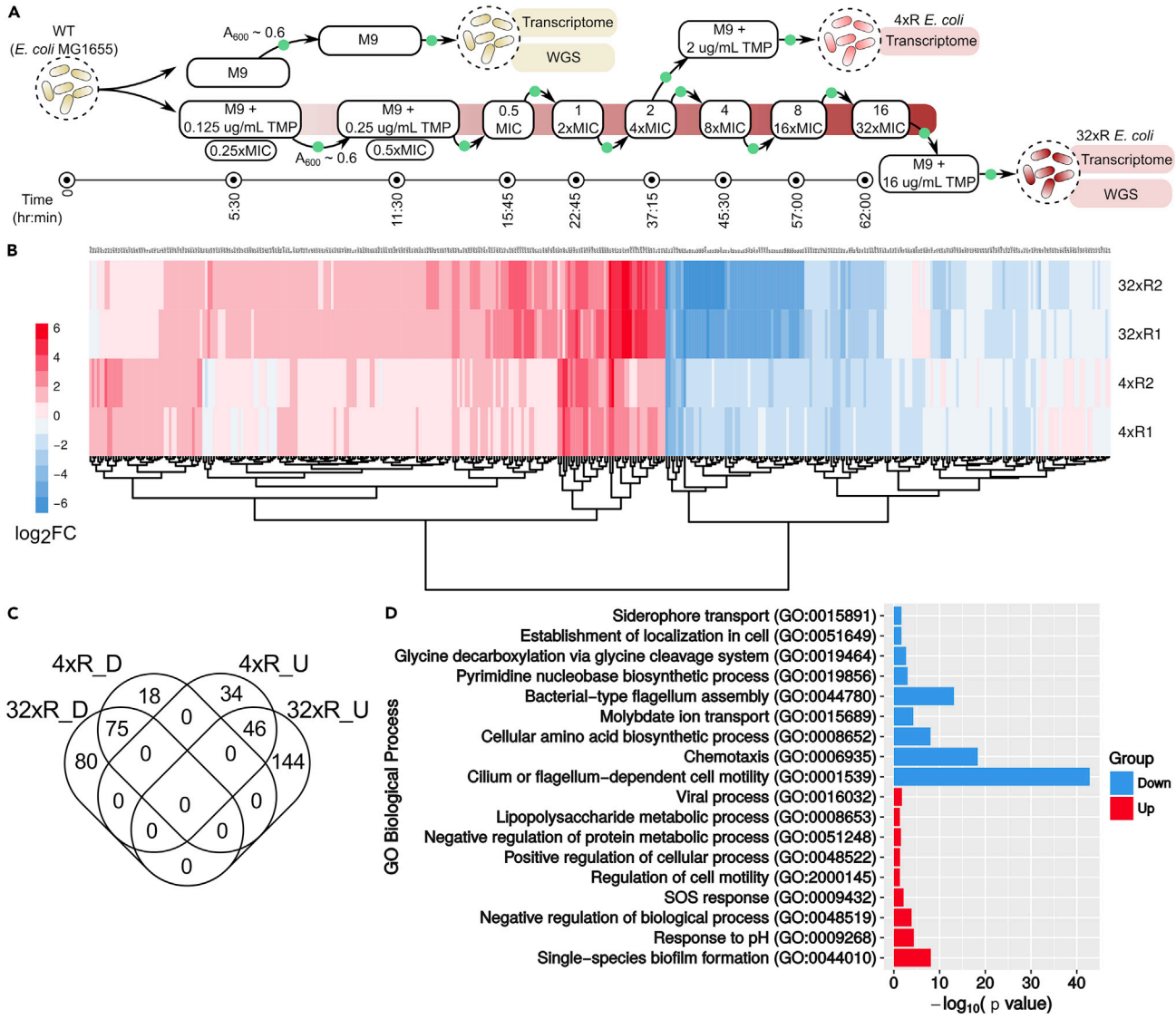

Figure 1. Laboratory-Evolved TMP-Resistant *E. coli* Exhibit Multiple Transcriptomic Changes

(A) Evolution of TMP-resistant 32xR *E. coli*: TMP-sensitive WT *E. coli* were adapted to TMP in a stepwise manner over 2.5 days. The adaptation was initiated by growing WT in sub-inhibitory (0.25xMIC) TMP concentration of 0.125 μg/mL to A_{600} ~ 0.6 (green filled circle) followed by inoculation in 2x TMP (0.25 μg/mL). This was done iteratively by doubling the concentration in each step till *E. coli* adapted to 16 μg/mL TMP. Line at the bottom indicates time after which the culture reached A_{600} ~ 0.6 in a particular concentration.

(B) log_2FC values of 397 DEGs in biological replicates of 4xR and 32xR *E. coli*. The FC of a gene is the mean of the FC of biological replicates of 4xR or 32xR. In general, FC is seen to be higher in 32xR as compared with 4xR.

(C) Common DEGs in 4xR and 32xR: 75 and 46 genes were commonly downregulated (D) and upregulated (U), respectively.

(D) Gene Ontology (GO) Biological Process enrichment of DEGs in 32xR *E. coli*: Biofilm formation, response to pH, and SOS response were significantly enriched in upregulated DEGs (red), whereas motility and amino acid biosynthesis were enriched in downregulated DEGs (blue).

biomarkers for tuberculosis (Padiadpu et al., 2016; Sambarey et al., 2017). In keeping with this, a functional interactome, *E. coli* protein-protein interaction network (EcPPIN), was constructed, integrated with transcriptome information, and used to study the cross talk underlying TMP resistance with the goal of identifying targetable components, if any.

EcPPIN was constructed using functional interaction data (regulatory, physical binding, metabolic, etc.) between 3,498 genes and had 24,542 edges obtained from public databases and the literature (see Transparent Methods). Furthermore, a condition-specific network, 32xNet, which captures gene expression

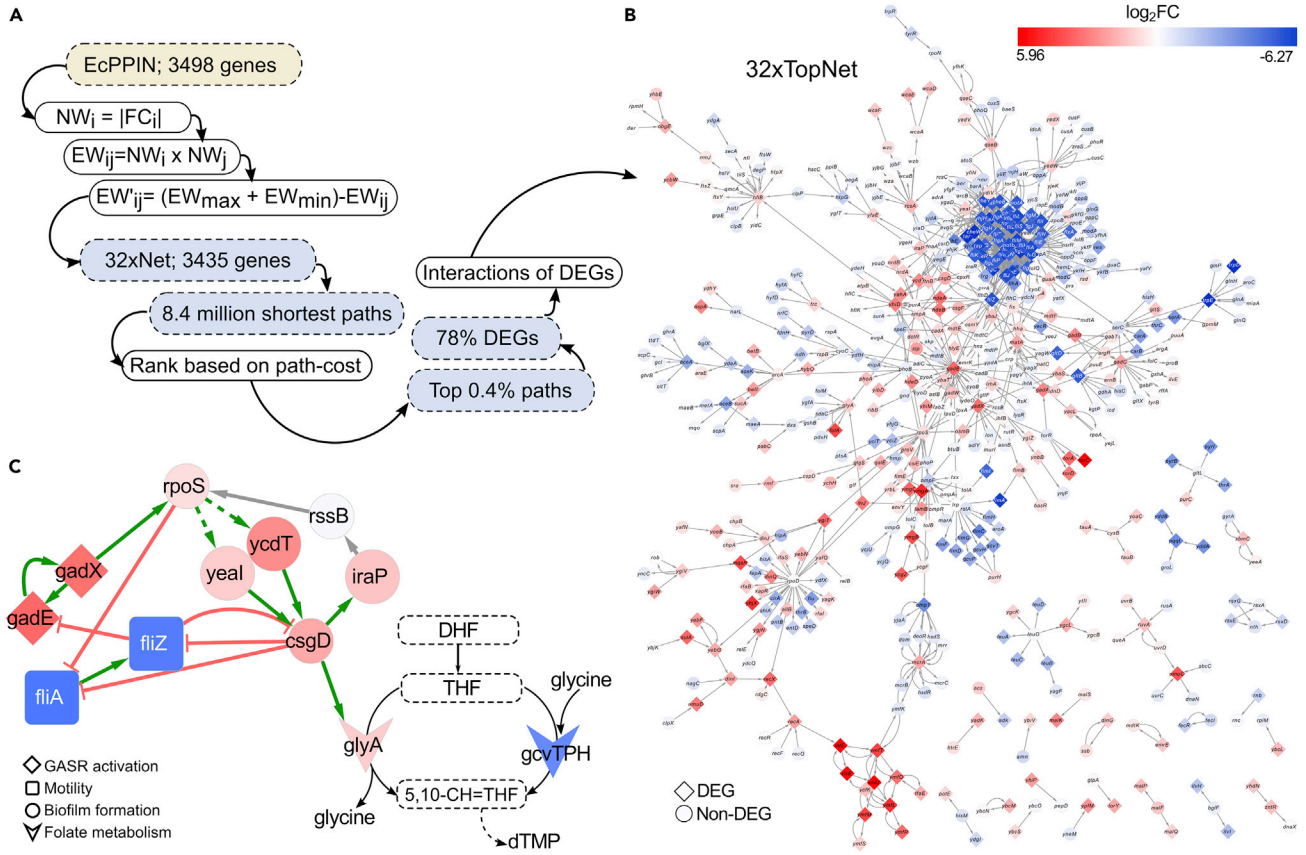

Figure 2. Cross Talk between Processes Perturbed by TMP Is Identified from 32xTopNet

(A) Flow chart showing steps involved in extraction of 32xTopNet from 32xNet.

(B) 32xTopNet: filled diamonds (DEGs) and circles (non-DEG genes) represent nodes and lines connecting them are knowledge-based functional interactions. The nodes are colored based on FC.

(C) Cross talk between processes perturbed by TMP viz. GASR, motility, biofilm, and folate metabolism inferred from the 32xTopNet. Genes belonging to each process are shown in a different shape. Like in (B), node colors signify extent of upregulation or downregulation.

perturbations associated with TMP resistance, was generated by integrating the differential transcriptome of WT and 32xR *E. coli* into EcPPIN (see Transparent Methods) (Figure 2A). Approximately 8.4 million shortest paths were detected in 32xNet and ranked based on normalized path costs (see Transparent Methods). A subset of top-ranked shortest paths that (1) was significantly enriched in DEGs (hypergeometric p value < 0.05) and (2) contained ≥75% of all observed DEGs was considered desirable for the identification of high-confidence resistance-associated perturbations. The top-ranked 0.4% shortest paths were observed to satisfy these criteria; enrichment p value = 0.003; 269 DEGs (78%) (Table S3). Since we were interested only in the interactions that are directly linked to or possibly impart TMP resistance, only the edges involving at least one DEG were considered, leading to the selection of 570 genes connected by 1,177 edges. Interestingly, most of the 1,177 edges, albeit a very small portion of the EcPPIN, formed a connected sub-network, 32xTopNet (Figure 2B). This connectedness indicated cross talk, i.e., individual processes influence each other and are perhaps orchestrated through common control elements.

Edge-weight-based clustering, which leverages the occurrence of dense connections between groups of genes belonging to the same process, was used to identify processes perturbed by TMP in the 32xTopNet (see Transparent Methods). Twenty-six clusters (C1 to C26) of size ≥ 4 (p value < 0.05) were obtained (Figure S2). Clusters were functionally annotated based on the annotations of its members as per EcoCyc (Keseler et al., 2011). Of the 26 clusters, genes in 11 (C2, C3, C6, C8, C10, C14, C16, C18, C21, C22, C26) were seen to be involved in stress-response processes, whereas genes in 5 others (C5, C13, C15, C17, C19) were metabolism related (Table 1). Amino acid biosynthesis, aerobic respiration, and glycine-cleavage complex

ID	p Value	Size	Member Genes	Annotation
C1	0	45	*cheA*, *cheB*, *cheW*, *cheY*, *cheZ*, *flgA*, *flgB*, *flgC*, *flgD*, *flgE*, *flgF*, *flgG*, *flgH*, *flgI*, *flgJ*, *flgK*, *flgL*, *flgM*, *flgN*, *flhB*, *fliA*, *fliC*, *fliD*, *fliE*, *fliF*, *fliG*, *fliH*, *fliI*, *fliJ*, *fliK*, *fliL*, *fliM*, *fliN*, *fliO*, *fliP*, *fliQ*, *fliS*, *fliT*, *fliZ*, *motA*, *motB*, *tap*, *tar*, *ycgR*, *yhjH*	Flagellar assembly and chemotaxis
C2	0.002	7	*uvrC*, ***umuC***, *dnaN*, *sbcC*, *uvrD*, ***ruvA***, *uvrB*	DNA repair
C3	0.004	7	***ygiW***, ***ygiV***, ***dinJ***, ***ygiT***, ***yafQ***, ***mqsR***, *hipA*	Biofilm regulation
C4	0.005	5	*sra*, ***rmf***, *cspD*, ***glgS***, *ychH*	
C5	0.005	8	*aceB*, *aceK*, *arcA*, ***betB***, ***betI***, ***hybO***, *maeA*, *ndh*	Aerobic respiration
C6	0.006	5	*ycgF*, ***ycgZ***, ***ymgA***, ***ymgB***, ***ymgC***	Biofilm architecture
C7	0.007	7	*dcm*, *deoR*, *hsdR*, *hsdS*, ***mcrA***, *ompT*, *yjaA*	DNA modification
C8	0.007	16	*csgD*, *fliZ*, ***gadA***, ***gadB***, ***gadC***, ***gadE***, ***gadX***, *gadW*, *gltB*, *gltD*, ***hdeA***, ***hdeB***, ***hdeD***, ***mdtE***, *slp*, ***yhiD***	Glutamate-dependent acid stress response
C9	0.011	4	*cysB*, *tauA*, *tauB*, *yoaC*	Sulfur provision
C10	0.011	6	***intE***, ***xisE***, ***ymfJ***, ***ymfM***, ***ymfT***	e14 prophage protein
C11	0.013	4	***frc***, *hyfA*, *hyfC*, *hyfD*	Hydrogenase subunit
C12	0.013	4	***aspA***, *fdnH*, *narL*, ***ydhY***	Nitrate/nitrite response
C13	0.015	4	*gcvH*, *gcvP*, *gcvT*, *purH*	Glycine cleavage
C14	0.015	4	*nth*, *rsxD*, *rsxE*, *rsxG*	SoxSR reducing system
C15	0.017	11	*argR*, *arnB*, *carA*, *carB*, *gdhA*, *gltB*, *gltD*, *gpmM*, *hisC*, *serA*, *serC*	Amino acid biosynthesis
C16	0.018	7	*fimI*, *ihfB*, ***matA***, *matC*, *yagW*, *yagX*, *ypdA*	Fimbrial-associated proteins
C17	0.019	6	*aceA*, *citT*, *gcl*, *ghrA*, *scpC*, *ttdT*	Glyoxylate metabolism and succinate transport
C18	0.019	6	*rpoS*, *ycgF*, ***ycgZ***, ***ymgA***, ***ymgB***, ***ymgC***	Biofilm architecture
C19	0.023	13	*argR*, ***gadA***, ***gadE***, *gadW*, ***gadX***, *gltB*, *gltD*, *hdeD*, *serC*, *slp*, ***ybaS***, ***ybaT***, ***yhiM***	Glutamate metabolism

Table 1. Clusters Identified in 32xTopNet

(Continued on next page)

ID	p Value	Size	Member Genes	Annotation
C20	0.024	11	*cheA*, *cheB*, *cheR*, *cheW*, *cheY*, *cheZ*, *fliA*, *motA*, *tap*, *tar*, *tsr*	Chemotaxis
C21	0.030	4	*nth*, *rsxA*, *rsxD*, *rsxE*	SoxSR reducing system
C22	0.030	4	*hipA*, ***mqsR***, ***ygiV***, ***ygiW***	Stress response
C23	0.030	6	*clpP*, *degP*, ***hflB***, ***obgE***, *rrmJ*, *yhbE*	
C24	0.032	9	*cheA*, *cheB*, *cheR*, *cheW*, *cheY*, *cheZ*, *tap*, *tar*, *tsr*	Chemotaxis
C25	0.040	16	*cheA*, *cheB*, *cheR*, *cheW*, *cheY*, *cheZ*, *flgK*, *flgL*, *fliA*, *fliS*, *motA*, *tap*, *tar*, *tsr*, *ycgR*, *yhjH*	Chemotaxis
C26	0.043	6	***rcsA***, *wcaA*, ***wcaE***, ***wcaF***, *wzc*, *yjbE*	Colanic acid biosynthesis

Table 1. Continued

Clusters of size 4 or more were identified in 32xTopNet. The first column provides the cluster ID in which the number specifies the rank. Clusters have been annotated based on the genes they contain. Annotation was possible only for clusters with majority of genes sharing a common ontology based on primary literature reports. Downregulated genes are underlined, and upregulated genes are shown in bold (log_2FC values in Table S1).

in the folate pathway were among the perturbed metabolic processes. SOS-response-DNA repair, glutamate-dependent acid-stress response (GASR), biofilm formation, superoxide detoxification, and e14 prophage were among the active stress response mechanisms. Some of these are of relevance to pathogenesis and host colonization. Using mouse models of human UTI, it has been reported that the induction of SOS response is important for survival of uropathogenic *E. coli* in the bladder epithelial cells of immunocompetent mice (Li et al., 2010). Similarly, biofilm formation has been linked to persistence and relapse of UTIs (Soto et al., 2006). We confirmed biofilm formation of the resistant *E. coli* using crystal violet staining and scanning electron microscopy. 32xR *E. coli* grown both in the absence and presence of 16 μg/mL TMP were seen to form more biofilm than the WT grown in the absence of TMP (Figure S3).

Most clusters contained genes belonging to a single process, whereas some represented multiple processes. Motility regulator *fliZ* was captured in both C1 and C8, which contain mainly motility and GASR genes, respectively (Table 1). FliZ negatively regulates GASR through the repression of GASR activator *gadE*, whereas, another GASR regulator, GadX, activates *rpoS*, which antagonizes *fliA* and *fliZ* expression (Figure 2C) (Dong et al., 2011; Pesavento and Hengge, 2012). Therefore, in the 32xR *E. coli*, the downregulation of *fliZ* can be linked to de-repression of GASR activator *gadE* and, as a consequence, induction of GASR. FliZ is a negative regulator of *csgD* expression, a transcription factor involved in biofilm formation and vice versa, whereas RpoS positively regulates *csgD* transcription through c-di-GMP (Figure 2C) (Ogasawara et al., 2011; Pesavento et al., 2008; Weber et al., 2006). In keeping with this, diguanylate cyclases (*yeaI*, *ycdT*) were found to be upregulated in 32xR *E. coli* (Table S1). Finally, and remarkably, a previously identified interaction between *csgD* and *glyA* (serine hydroxymethyltransferase) seen in the 32xTopNet highlighted the cross talk between a stress-response mechanism, i.e., biofilm formation and the folate pathway (Figure 2C) (Chirwa and Herrington, 2003).

Emergent Vulnerability in TMP-Resistant *E. coli*

GlyA catalyzes the formation of 5,10-methylene tetrahydrofolate (5,10-mTHF) and glycine from serine and THF. The glycine cleavage complex (GcvTPH) (found in C13) also synthesizes 5,10-mTHF from THF; however, it utilizes glycine instead of serine. The 5,10-mTHF produced by these reactions is used for the synthesis of dTMP by ThyA. Both GlyA and GcvTPH lie directly downstream of FolA in the folate pathway (Figure 2C). A recent study by Minato et al. showed that the deletion of either *gcv* or *glyA* did not improve

susceptibility of WT *E. coli* to TMP (Minato et al., 2018). This could be because these two reactions are functionally redundant. Since *gcvTPH* was downregulated in the 32xR *E. coli* (Table S1), the data suggested that the resistant *E. coli* critically depend on *glyA* for production of 5,10-mTHF and subsequently the nucleotides and DNA. Since this dependence on GlyA is unique to the resistant strains, we hypothesized that it is a new vulnerability that has emerged in association with TMP resistance and that *E. coli* devoid of GlyA activity cannot sustain resistance. To confirm this, we first generated *glyA* knockouts of the 32xR1 and 32xR2 *E. coli* (Figure S4). The knockouts were observed to grow satisfactorily (Figure S4). The MIC of TMP for 32xR1:Δ*glyA* and 32xR2:Δ*glyA* was recorded to be 8 and 4 μg/mL, respectively, which translated to a 32-fold decrease in MIC for 32xR2 and more than 100-fold decrease in MIC for 32xR1. Furthermore, to test if our findings hold true for clinical strains of pathogenic *E. coli*, we created a *glyA* knockout of an MDR strain of uropathogenic *E. coli* isolated from a patient with acute UTI. This clinical isolate (CI) was resistant to therapeutic concentrations of ampicillin, piperacillin/tazobactam, cephamycin, cephalosporin antibiotics, cotrimoxazole, ciprofloxacin, and norfloxacin (sensitivity profiling obtained from the hospital repository). It was resistant to TMP with an MIC of 1,024 μg/mL and showed an upregulation GASR, *csgD*, and *glyA* as compared with WT even in the absence of TMP. Like the 32xR1 and 32xR2 *E. coli*, this clinical isolate exhibited slight but significant upregulation of *glyA* and *folA* and downregulation of *gcvT* in the presence of 16 μg/mL and CI:Δ*glyA* showed no growth defect (Tables S1 and S4, Figure S5). However, it did not contain mutations in the chromosomal *folA* indicating that the high resistance could be due to the presence of plasmid-borne naturally resistant dihydrofolate reductase enzymes like in most clinical isolates and not the mutation/overexpression of chromosomal *folA* like in 32xR *E. coli*. Remarkably, the MIC of TMP for CI:Δ*glyA* was also observed to be 8 μg/mL, which, like for 32xR1, translated to a ~100-fold decrease. Collectively, these data showed that the dependence on *glyA* is indeed an emergent vulnerability associated with TMP resistance.

Co-targeting GlyA Retards Acquisition of TMP Resistance

We observed that the upregulation of *glyA* and biofilm formation occurs even when WT is grown in sub-inhibitory concentrations of TMP (Figure S6). Specifically, WT grown at 0.125 μg/mL (0.25 x MIC) TMP showed ~3-fold higher expression of *glyA* (as compared with WT grown in absence of TMP) with concomitant downregulation of *gcvT* suggesting that GlyA activity is necessary to combat TMP stress (Table S4). Therefore, we asked if GlyA is necessary for adaptation to TMP. Toward this, we carried out a comparative evolution experiment with *E. coli* K12 BW25113 and BW25113:Δ*glyA* as previously described (Zampieri et al., 2017). The experiment was performed to simulate the adaptation to TMP over the course of a standard UTI treatment. (Note: Depending on the severity of the infection and the Food and Drug Administration's [FDA] guidelines [https://www.accessdata.fda.gov/drugsatfda_docs/label/2002/17943s16lbl.pdf], TMP is prescribed for 3–14 days with dosage every 12 [100 mg] or 24 h [200 mg]. As per the FDA reports, mean peak serum and urine concentrations of 1–2.5 and 30–160 μg/mL, respectively, are achieved 1–4 h after oral administration of a single dose of 100 mg.) Each replicate was exposed to different concentrations of TMP for 12 h post-incubation; *E. coli* growing at the highest concentration were selected for further propagation. Sub-culturing was carried out every 12 h over a period of 14 days. For each 12h period, for each strain, growth observed (A_{600}) in a well containing the replicate grown in absence of TMP was considered as the positive control (Figure 3A). The well from which the bacteria were to be selected for subsequent inoculation had to have $A_{600} \geq A_{600}$ of the positive control (Figure 3A). To account for the differences in the growth rate between BW25113 and BW25113:Δ*glyA*, resistance gained at equivalent number of generations was compared.

Both strains completed ~180 generations over 14 days, of which ~120 generations were completed over 10 days (Table S5). The average number of generations completed every 12 h was similar too (Table S5). On the fifth day (~60 generations) the maximum concentration at which BW25113 and BW25113:Δ*glyA* were observed to grow were 8 and 2 μg/mL, respectively (Figure 3B). This suggested that BW25113:Δ*glyA* could still be inhibited by the physiologically encountered concentration of TMP, whereas BW25113 could not. In the period between ~100 and 140 generations (~8–10.5 days), BW25113 was significantly more TMP resistant as compared with BW25113:Δ*glyA* (Figure 3C). After 11.5 days, ≥50% BW25113:Δ*glyA* replicates acquired resistance to ≥4 μg/mL, which is higher than the therapeutic serum concentration. However, this lies significantly outside the typical length of TMP treatment regimens for uncomplicated UTIs, i.e., 3 days (Jancel and Dudas, 2002). In summary, the experiment suggested that, in comparison with BW25113, BW25113:Δ*glyA* show delayed acquisition of low levels of TMP resistance.

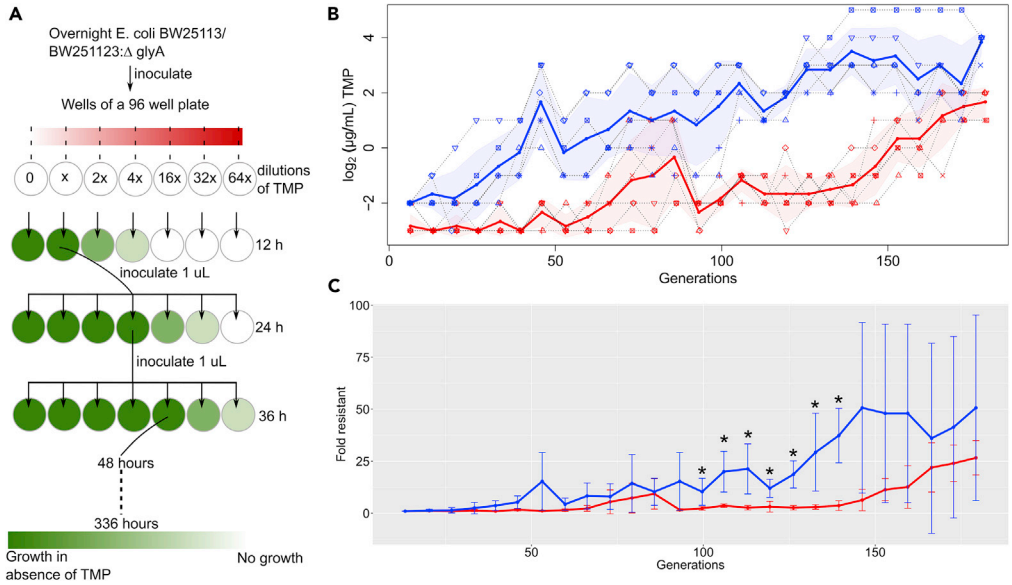

Figure 3. Comparative Evolution Shows Slower Adaptation to TMP in Absence of *glyA*

(A) Comparative evolution experiment schematic: Dilutions of TMP were prepared in a 96-well plate and inoculated with overnight cultures of BW25113 or BW25113:Δ*glyA*. Culture from well with the highest TMP concentration was used for inoculating plate for the next day provided growth in that well was comparable with growth in the absence of TMP ($A_{600} \geq A_{600}$ of corresponding well without TMP).

(B) Adaptation trajectories to TMP in six biological replicates of BW25113 (blue) and its corresponding BW25113:Δ*glyA* (red) over ~180 generations are shown. Each point for a particular number of generations for a particular replicate represents the maximum TMP concentration at which satisfactory growth ($A_{600} \geq A_{600}$ of corresponding well without TMP) was observed. Adaptation trajectory of each replicate is shown in a dotted line connecting the points for that replicate across all generations. The mean adaptation trajectory for BW25113 or BW25113:Δ*glyA* is shown in a solid line.

(C) Plot shows the mean resistance gained at a particular number of generations for BW25113 or BW25113:Δ*glyA*. For each replicate, the ratio of concentration at which it grows after a particular number of generations and the concentration at which it grew on the first day (after ~12 generations) is calculated. Thus, each ratio represents the fold increase in resistance. Six ratios are obtained per strain and the mean ± SD of these ratios is shown for a particular number of resistant. Since the number of generations completed every 12 h is roughly the same for the two strains, for the purpose of comparison, the BW25113 ratios have also been plotted using the number of generations obtained for BW25113:Δ*glyA*. Between ~100 and 140 generations (~8–10.5 days), BW25113 (blue) is significantly more resistant to TMP than BW25113:Δ*glyA* (red) (p value < 0.05; indicated by *).

Concluding Remarks

Although overexpression of a resistant DHFR directly provides TMP resistance in 32xR *E. coli*, the concomitant alterations in expression of a large number of genes (~8% of the genome) indicates that TMP resistance is a multifaceted response. Integration of the differential transcriptome of WT and 32xR *E. coli* into EcPPIN and an unbiased mining of the condition-specific network 32xNet not only revealed the cross talk between genes involved in different stress response and metabolic pathways perturbed by TMP but also led to the identification of an emergent vulnerability-critical dependence on GlyA. This vulnerability emerges from the multipronged role of GlyA, which ensures uninterrupted DNA synthesis via 5,10-mTHF and dTMP production, protein synthesis, and curli production through glycine production. We show that, even in the presence of primary resistance mechanisms such as the overexpression of a mutant chromosomal DHFR and associated beneficial perturbations viz. activation of the SOS/DNA-repair response and biofilm formation and, possibly, plasmid-borne naturally resistant dihydrofolate reductases in the clinical isolate, deletion of *glyA* rescues sensitivity to TMP to a large extent. The success of *glyA* as a target is attributable to its position in the folate pathway, i.e., downstream of THF biosynthesis where most dihydrofolate reductase activity-based resistance mechanisms functionally converge. Previous studies show that SHMT (GlyA) knockdown induces apoptosis in lung cancer cells and challenges viability in *P. falciparum* (Paone et al., 2014; Pornthanakasem et al., 2012). Since we also show that targeting this resistance-associated emergent vulnerability decelerates the acquisition of resistance in wild-type TMP-sensitive *E. coli*, a GlyA inhibitor used in combination with TMP presents a promising strategy for treating UPEC UTIs.

Limitations of the Study

1. Although *E. coli* lacking *glyA* show slower adaptation to TMP, it is possible that more than one TMP-adaptation strategy exist and that the outcomes of evolution *in vivo* and *in vitro* (in a controlled laboratory environment) are different.
2. Resistance mechanisms in laboratory-evolved and clinical *E. coli* may differ. It is difficult to predict the outcome of targeting *glyA* in clinical strains that are resistant to TMP through non-folate pathway-dependent mechanisms, e.g., efflux pumps and drug avoidance via biofilm formation.
3. Prediction of the cross talk between processes depends on the topology of the network and is, therefore, limited by the knowledge of functional interactions in *E. coli*.

METHODS

All methods can be found in the accompanying Transparent Methods supplemental file.

DATA AND CODE AVAILABILITY

The accession ID of the microarray expression data reported in this paper is ArrayExpress: E-MTAB-6536. R code for analysis of expression data, EcPPIN, and toy networks and scripts for weighted network generation and shortest path computation are made available in a supplementary zipped folder.

SUPPLEMENTAL INFORMATION

Supplemental Information can be found online at https://doi.org/10.1016/j.isci.2020.100986.

ACKNOWLEDGMENTS

Kapudeep Karmakar (Dept. of Microbiology and Cell Biology, Indian Institute of Science) is acknowledged for guidance with SEM. Srinivasan (Advanced Facility for Microscopy and Microanalysis, Indian Institute of Science) is acknowledged for technical assistance with SEM image acquisition. Deepesh Nagarajan (Department of Biochemistry, Indian Institute of Science) is acknowledged for acquiring and providing clinical isolate of uropathogenic *E. coli* from Ramaiah Memorial Hospital, Bangalore, India. We gratefully acknowledge support from the Ministry of Human Resource Development, Government of India, through the Institution of Eminence program and also from the Department of Biotechnology, Ministry of Science and Technology, Government of India in the form of a DBT-IISc partnership grant.

AUTHOR CONTRIBUTIONS

A.B. and N.C. conceptualized the study. D.C planned the validation experiments. A.B. developed the resistant *E. coli* and performed all computational analyses. A.D. and G.C. carried out the comparative evolution experiment, qPCR (D.S.), and knockout generation. N.C. and D.C. acquired funding for the research. A.B. and N.C. wrote the manuscript with inputs from A.D. and D.C. All authors read and approved the final manuscript.

DECLARATION OF INTERESTS

N.C. is a co-founder of qBiome Pvt. Ltd., which had no role in this manuscript.

Received: September 24, 2019
Revised: February 9, 2020
Accepted: March 10, 2020
Published: April 24, 2020

REFERENCES

Acar, J.F., Goldstein, F., and Chabbert, Y.A. (1973). Synergistic activity of trimethoprim-sulfamethoxazole on gram-negative bacilli: observations in vitro and in vivo. J. Infect. Dis. *128*, 470–477.

Chirwa, N.T., and Herrington, M.B. (2003). CsgD, a regulator of curli and cellulose synthesis, also regulates serine hydroxymethyltransferase synthesis in *Escherichia coli* K-12. Microbiology *149*, 525–535.

Dong, T., Yu, R., and Schellhorn, H. (2011). Antagonistic regulation of motility and transcriptome expression by RpoN and RpoS in *Escherichia coli*. Mol. Microbiol. *79*, 375–386.

Erickson, K.E., Otoupal, P.B., and Chatterjee, A. (2017). Transcriptome-level signatures in gene expression and gene expression variability during bacterial adaptive evolution. MSphere *2*.

Flensburg, J., and Sköld, O. (1987). Massive overproduction of dihydrofolate reductase in

bacteria as a response to the use of trimethoprim. Eur. J. Biochem. *162*, 473–476.

Huovinen, P., Sundström, L., Swedberg, G., and Sköld, O. (1995). Trimethoprim and sulfonamide resistance. Antimicrob. Agents Chemother. *39*, 279–289.

Imamovic, L., and Sommer, M.O.A. (2013). Use of collateral sensitivity networks to design drug cycling protocols that avoid resistance development. Sci. Transl. Med. *5*, 204ra132.

Jancel, T., and Dudas, V. (2002). Management of uncomplicated urinary tract infections. West. J. Med. *176*, 51–55.

Kasanen, A., and Sundquist, H. (1982). Trimethoprim alone in the treatment of urinary tract infections: eight years of experience in Finland. Rev. Infect. Dis. *4*, 358–365.

Keseler, I.M., Collado-Vides, J., Santos-Zavaleta, A., Peralta-Gil, M., Gama-Castro, S., Muñiz-Rascado, L., Bonavides-Martinez, C., Paley, S., Krummenacker, M., Altman, T., et al. (2011). EcoCyc: a comprehensive database of *Escherichia coli* biology. Nucleic Acids Res. *39*, D583–D590.

Kwon, Y.K., Higgins, M.B., and Rabinowitz, J.D. (2010). Antifolate-induced depletion of intracellular glycine and purines inhibits thymineless death in E. coli. ACS Chem. Biol. *5*, 787–795.

Li, B., Smith, P., Horvath, D.J., Romesberg, F.E., and Justice, S.S. (2010). SOS regulatory elements are essential for UPEC pathogenesis. Microbes Infect. *12*, 662–668.

Minato, Y., Dawadi, S., Kordus, S.L., Sivanandam, A., Aldrich, C.C., and Baughn, A.D. (2018). Mutual potentiation drives synergy between trimethoprim and sulfamethoxazole. Nat. Commun. *9*, 1003.

Mitosch, K., Rieckh, G., and Bollenbach, T. (2017). Noisy response to antibiotic stress predicts subsequent single-cell survival in an acidic environment. Cell Syst. *4*, 393–403.e5.

Mohan, A., Bhosle, A., and Chandra, N. (2015). Complete genome sequences of an *Escherichia coli* laboratory strain and trimethoprim-resistant (TMP32XR) mutant strains. Genome Announc. *3*, e01434–15.

Ogasawara, H., Yamamoto, K., and Ishihama, A. (2011). Role of the biofilm master regulator CsgD in cross-regulation between biofilm formation and flagellar synthesis. J. Bacteriol. *193*, 2587–2597.

Padiadpu, J., Baloni, P., Anand, K., Munshi, M., Thakur, C., Mohan, A., Singh, A., and Chandra, N. (2016). Identifying and tackling emergent vulnerability in drug-resistant mycobacteria. ACS Infect. Dis. *2*, 592–607.

Paone, A., Marani, M., Fiascarelli, A., Rinaldo, S., Giardina, G., Contestabile, R., Paiardini, A., and Cutruzzolà, F. (2014). SHMT1 knockdown induces apoptosis in lung cancer cells by causing uracil misincorporation. Cell Death Dis. *5*, e1525.

Pesavento, C., and Hengge, R. (2012). The global repressor FliZ antagonizes gene expression by σS-containing RNA polymerase due to overlapping DNA binding specificity. Nucleic Acids Res. *40*, 4783–4793.

Pesavento, C., Becker, G., Sommerfeldt, N., Possling, A., Tschowri, N., Mehlis, A., and Hengge, R. (2008). Inverse regulatory coordination of motility and curli-mediated adhesion in *Escherichia coli*. Genes Dev. *22*, 2434–2446.

Pornthanakasem, W., Kongkasuriyachai, D., Uthaipibull, C., Yuthavong, Y., and Leartsakulpanich, U. (2012). Plasmodium serine hydroxymethyltransferase: indispensability and display of distinct localization. Malar. J. *11*, 387.

Sambarey, A., Devaprasad, A., Mohan, A., Ahmed, A., Nayak, S., Swaminathan, S., D'Souza, G., Jesuraj, A., Dhar, C., Babu, S., et al. (2017). Unbiased identification of blood-based biomarkers for pulmonary tuberculosis by modeling and mining molecular interaction networks. EBioMedicine *15*, 112–126.

Sanchez, G.V., Master, R.N., Karlowsky, J.A., and Bordon, J.M. (2012). In vitro antimicrobial resistance of urinary *Escherichia coli* isolates among U.S. outpatients from 2000 to 2010. Antimicrob. Agents Chemother. *56*, 2181–2183.

Sangurdekar, D.P., Zhang, Z., and Khodursky, A.B. (2011). The association of DNA damage response and nucleotide level modulation with the antibacterial mechanism of the anti-folate drug trimethoprim. BMC Genomics *12*, 583.

Schulz, M., and Schmoldt, A. (2003). Therapeutic and toxic blood concentrations of more than 800 drugs and other xenobiotics. Pharmazie *58*, 447–474.

Seputienė, V., Povilonis, J., Ruzauskas, M., Pavilonis, A., and Suziedėlienė, E. (2010). Prevalence of trimethoprim resistance genes in *Escherichia coli* isolates of human and animal origin in Lithuania. J. Med. Microbiol. *59*, 315–322.

Soto, S.M., Smithson, A., Horcajada, J.P., Martinez, J.A., Mensa, J.P., and Vila, J. (2006). Implication of biofilm formation in the persistence of urinary tract infection caused by uropathogenic *Escherichia coli*. Clin. Microbiol. Infect. *12*, 1034–1036.

Toprak, E., Veres, A., Michel, J.-B., Chait, R., Hartl, D.L., and Kishony, R. (2011). Evolutionary paths to antibiotic resistance under dynamically sustained drug selection. Nat. Genet. *44*, 101–105.

Volpato, J.P., and Pelletier, J.N. (2009). Mutational "hot-spots" in mammalian, bacterial and protozoal dihydrofolate reductases associated with antifolate resistance: sequence and structural comparison. Drug Resist. Updat. *12*, 28–41.

Wambaugh, M.A., Shakya, V.P.S., Lewis, A.J., Mulvey, M.A., and Brown, J.C.S. (2017). High-throughput identification and rational design of synergistic small-molecule pairs for combating and bypassing antibiotic resistance. PLoS Biol. *15*, e2001644.

Weber, H., Pesavento, C., Possling, A., Tischendorf, G., and Hengge, R. (2006). Cyclic-di-GMP-mediated signalling within the sigma network of *Escherichia coli*. Mol. Microbiol. *62*, 1014–1034.

White, P.A., McIver, C.J., Deng, Y., and Rawlinson, W.D. (2000). Characterisation of two new gene cassettes, aadA5 and dfrA17. FEMS Microbiol. Lett. *182*, 265–269.

Zampieri, M., Enke, T., Chubukov, V., Ricci, V., Piddock, L., and Sauer, U. (2017). Metabolic constraints on the evolution of antibiotic resistance. Mol. Syst. Biol. *13*, 917.

Zhou, A., Kang, T.M., Yuan, J., Beppler, C., Nguyen, C., Mao, Z., Nguyen, M.Q., Yeh, P., and Miller, J.H. (2015). Synergistic interactions of vancomycin with different antibiotics against *Escherichia coli*: trimethoprim and nitrofurantoin display strong synergies with vancomycin against wild-type E. coli. Antimicrob. Agents Chemother. *59*, 276–281.

iScience, Volume *23*

Supplemental Information

A Strategic Target Rescues Trimethoprim Sensitivity in *Escherichia coli*

Amrisha Bhosle, Akshay Datey, Giridhar Chandrasekharan, Deepshikha Singh, Dipshikha Chakravortty, and Nagasuma Chandra

Supplementary Information

Supplementary Figures

Figure S1: Growth of WT and laboratory-evolved TMP-resistant 32xR *E. coli* [related to Figure 1]: Growth curves of 32xR1 and 32xR2 *E. coli* in presence (-T) and absence of 16 µg/mL TMP; and respective *E. coli* K12 MG1655 parents (WT1 and WT2) are shown. A_{600} recorded at each hour is shown as mean ± SD. The 32xR strains grow only marginally slower as compared to their respective WT parents and there is no significant difference in growth in presence and absence of 16 µg/mL TMP.

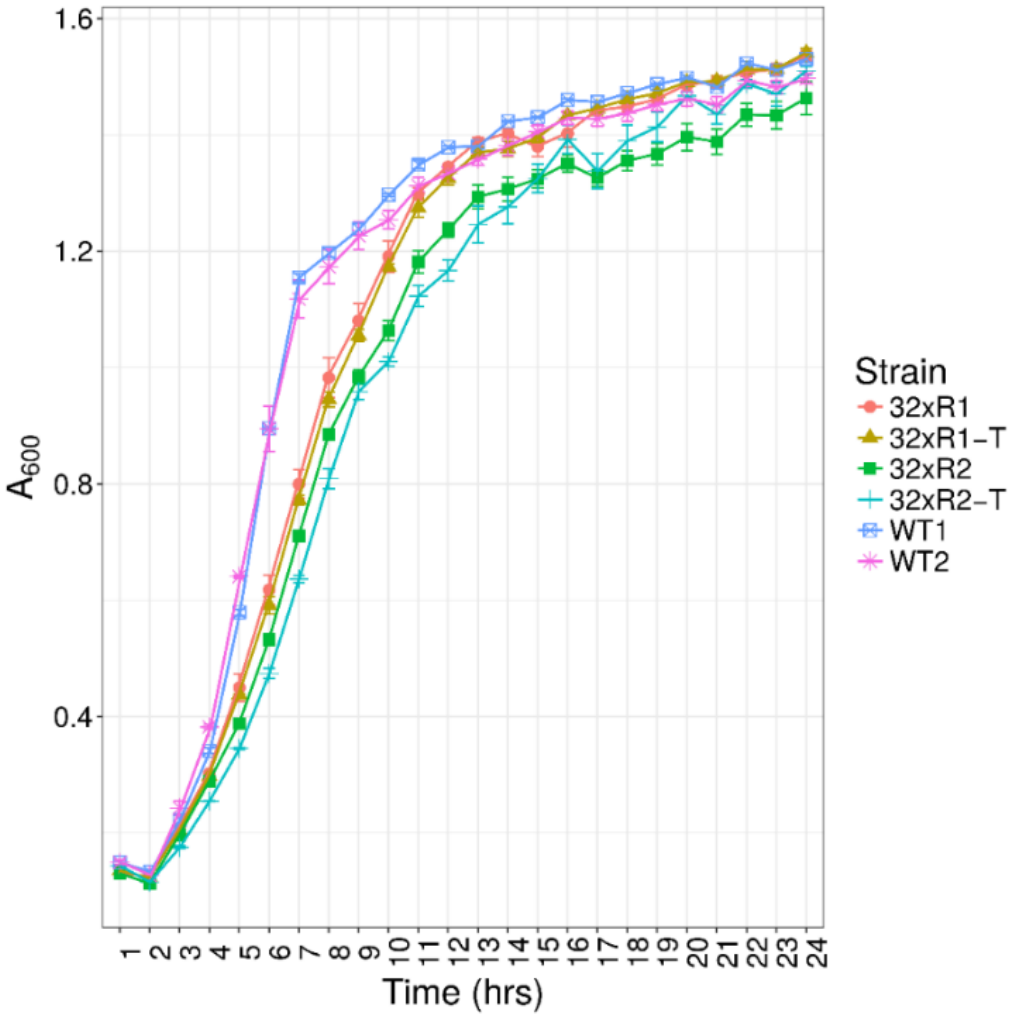

Figure S2: Clusters identified in 32xTopNet [related to Table 1]: ClusterONE (Clustering with Overlapping Neighbourhood Expansion (Nepusz et al., 2012)) was used to identify clusters based on edge-weights. ClusterONE identifies clusters with overlapping nodes. For example, if a gene pair A-B has a higher edge-weight and so does the pair A-C but not the pair B-C, then gene A will be observed in two clusters, one which has gene B and its interactions and another which has gene C and its interactions. Therefore, multiple clusters containing the same genes are observed. 26 clusters were identified.

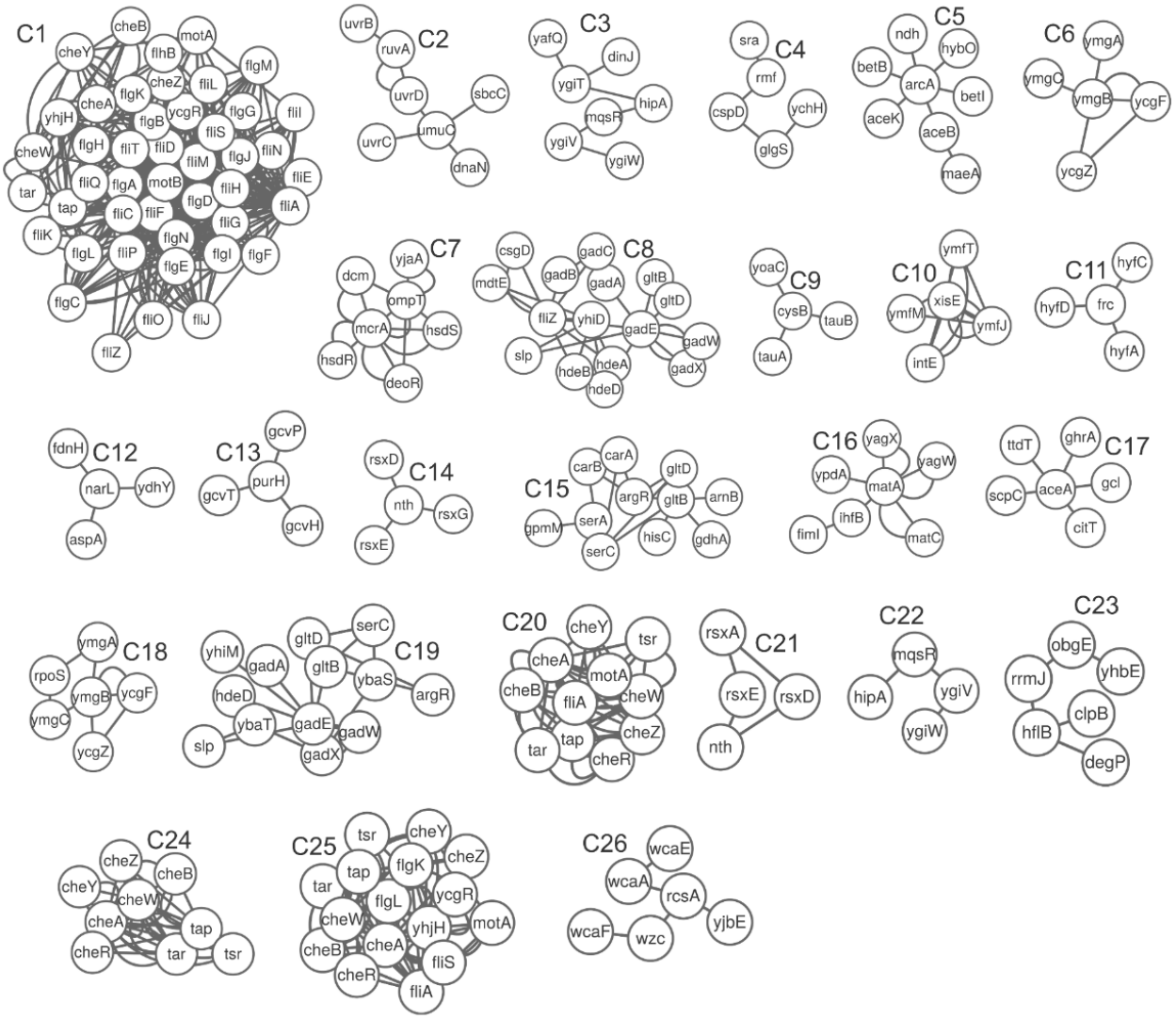

Figure S3: Biofilm formation [related to Table 1, Figure 1 and Figure 2]: (a) Biofilm quantification by crystal violet staining (A_{590} data plotted as mean ± SD) showed that biofilm production by the 32xR strains both in the absence and presence of 16 µg/mL TMP was higher as compared to WT. (b) Scanning electron microscopy (SEM) images at 4000X of *E. coli* biofilms showed that 32xR *E. coli* clump together in a biofilm matrix whereas WT appear mostly as separate cells. The clumping in each field is demarcated for ease of viewing.

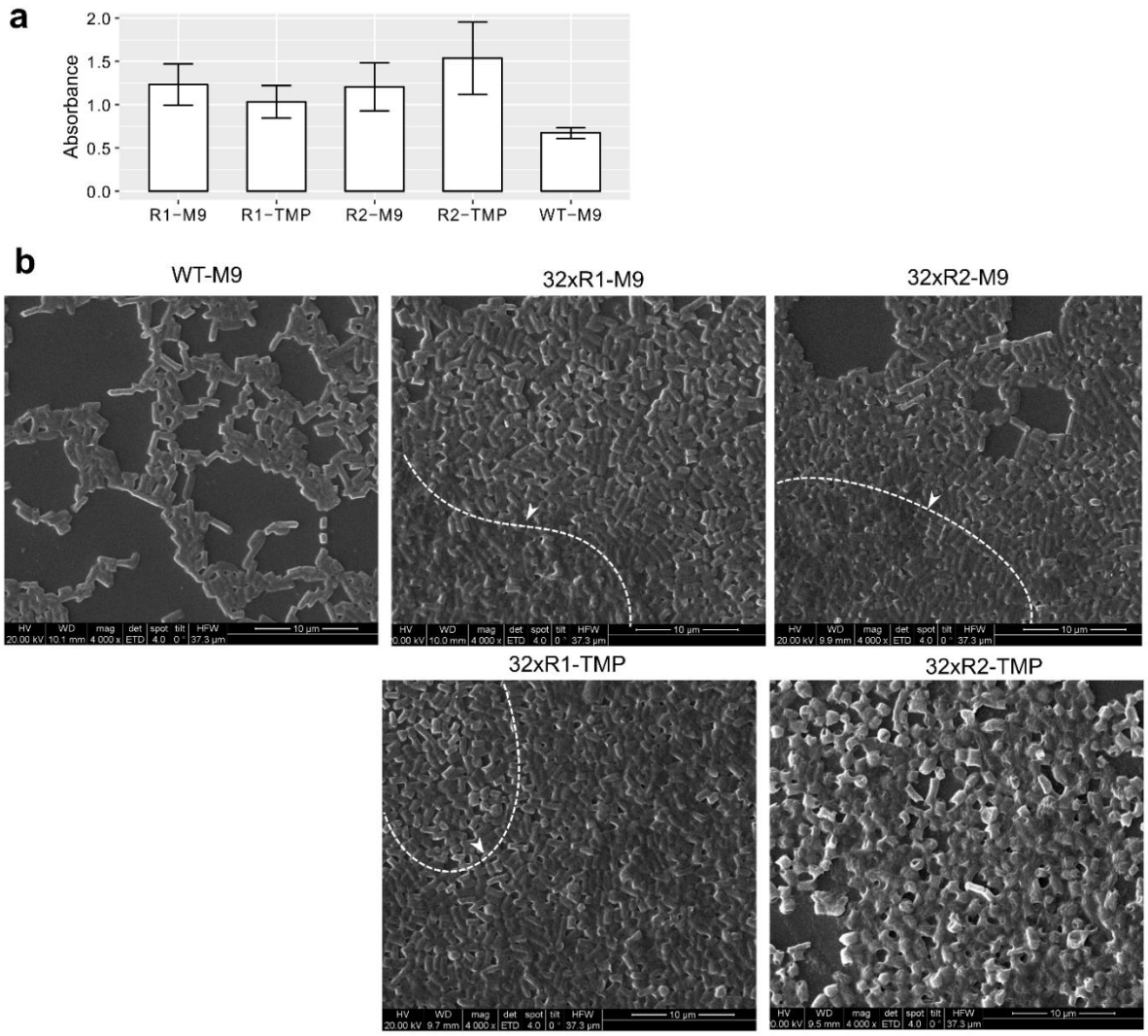

Figure S4: Confirmation of *glyA* knockouts [related to Figure 2C]

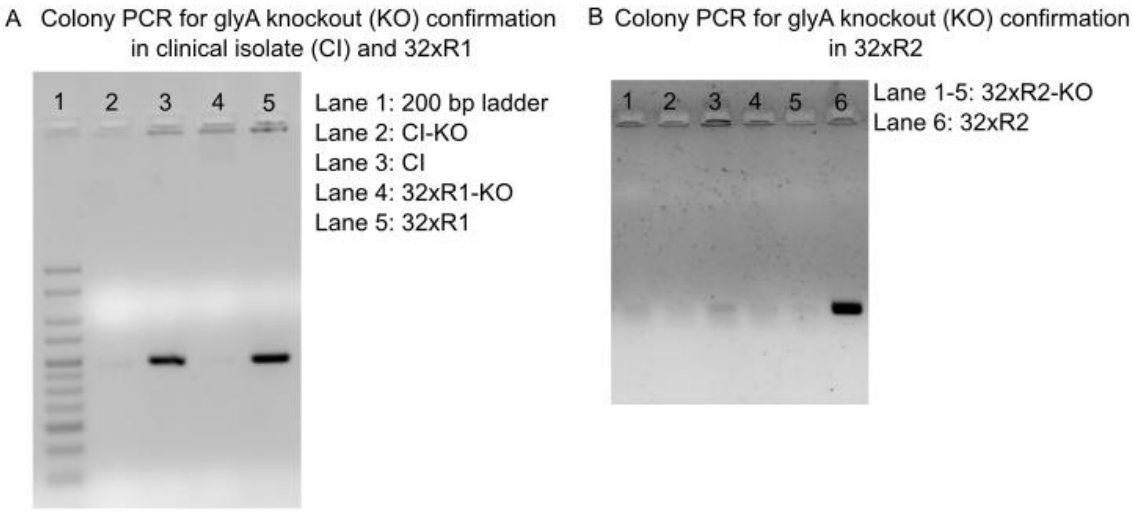

Figure S5: Growth curves of 32xR1, 32xR2 and CI and their respective *glyA* knockouts [related to Figure 2]: Growth in the absence of TMP was profiled for 32xR strains and clinical isolate-CI (red) and their respective Δ*glyA* (black) over 24 hours. $\log_{10}$(CFU/mL) is the average of two biological replicates.

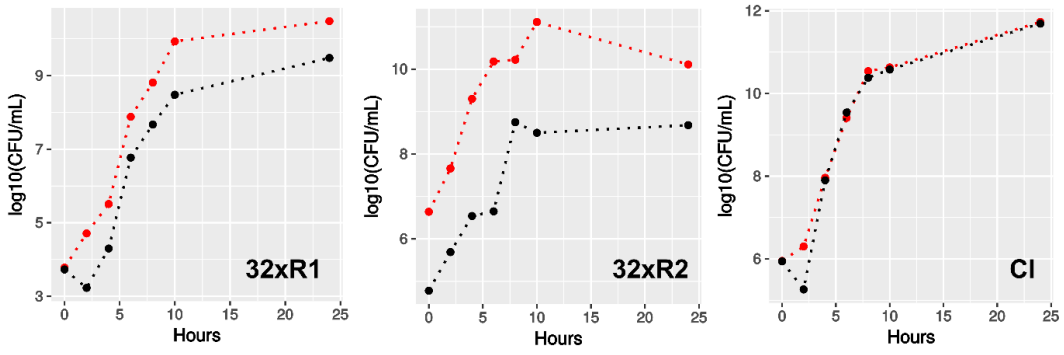

Figure S6: Biofilm formation by WT in response to TMP stress [related to Figures 1 and Figure 3]: Biofilm quantification by crystal violet staining (A_{590} data plotted as mean ± SD) showed that biofilm production in WT increases upon exposure to sub-inhibitory, but stress inducing, TMP concentrations i.e. 0.25xMIC (0.125 µg/mL) and 0.5xMIC (0.25 µg/mL) (p-value < 0.01).

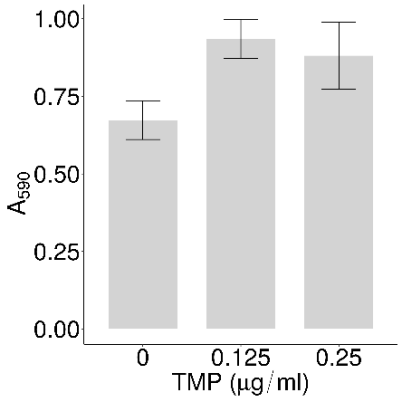

Supplementary Tables

Table S1: DEGs in the 32xR *E. coli* [related to Figure 1]: log_2FC is the mean log_2FC for the 32xR1 and 32xR2 strains

Gene	log_2FC	Gene	log_2FC	Gene	log_2FC	Gene	log_2FC	Gene	log_2FC
ais	1.81	*recN*	1.76	*yeeD*	2.55	*codB*	-1.99	*maeA*	-1.1
allB	1.61	*recX*	3.49	*yeeE*	2.88	*cyaA*	-1.21	*metE*	-2.01
aphA	1.41	*rfaB*	1.29	*yegJ*	1.33	*cybB*	-1.75	*mipA*	-1.06
aspA	2.82	*rfaI*	1.02	*yfaE*	1.18	*entD*	-1.24	*mntH*	-1.17
betB	1.87	*rfaS*	1.21	*yfbP*	1.57	*fdnH*	-1.19	*modA*	-1.73
betI	2.4	*rhsA*	1.32	*yfcV*	1.53	*fecR*	-1.18	*modB*	-1.63
cadA	1.02	*rhsD*	2.61	*yfdY*	1.21	*fepA*	-1.54	*modC*	-1.87
csiE	1.71	*ribB*	1.06	*ygcK*	1.21	*fhuE*	-2.04	*modF*	-1.2
dinG	1.26	*rmf*	1.78	*ygcL*	2.06	*fimA*	-5.72	*motA*	-4.91
dinI	2.13	*ruvA*	1.56	*ygcO*	1.03	*fimC*	-3.58	*motB*	-5.29
dinJ	1.33	*sbmC*	1.54	*ygdQ*	1.02	*fimD*	-2.42	*ndh*	-1.44
dinQ	2.83	*sfmD*	1.3	*ygiS*	2.9	*fimF*	-2.66	*ompF*	-1.35
emrE	1.35	*smpA*	1.06	*ygiT*	3.47	*fimG*	-2.62	*ompT*	-3.47
fimB	1.31	*sucA*	1.34	*ygiV*	1.24	*fimH*	-2.02	*oppA*	-1.17
fimE	1.21	*sulA*	3.57	*ygiW*	2.3	*fimI*	-4.58	*pntB*	-1.45
folA	4.27	*tauA*	1.16	*ygiZ*	1.02	*fiu*	-2.84	*pqqL*	-3.6
frc	1.1	*tauB*	1.01	*ygjN*	2.46	*flgA*	-4.89	*pyrB*	-3.06
ftnB	1.6	*tdcB*	1.33	*yhdN*	1.43	*flgB*	-5.87	*pyrD*	-1.53
gadA	2.82	*tfaE*	1.9	*yhhH*	1.42	*flgC*	-5.85	*pyrI*	-3
gadB	2.79	*tisA*	4.8	*yhiD*	3.02	*flgD*	-5.94	*rnb*	-1.11
gadC	2.15	*tisB*	5.07	*yhiM*	2.34	*flgE*	-5.55	*rsxD*	-1.1
gadE	3.55	*torA*	3.53	*yhiP*	2.35	*flgF*	-5.63	*rsxE*	-1.11
gadX	3.37	*torC*	5.91	*yhjX*	4.66	*flgG*	-5.31	*rsxG*	-1.06
galE	1.89	*torD*	3.09	*yibA*	1.17	*flgH*	-4.87	*sapA*	-1.33
glgS	1.33	*torY*	2.07	*yibD*	1.88	*flgI*	-4.69	*serA*	-3.03
gltS	1.42	*tyrP*	1.01	*yibT*	1.42	*flgJ*	-4.68	*shiA*	-1.18
glyA	1.26	*umuC*	3.95	*yibV*	2.22	*flgK*	-5.19	*speD*	-1.36
guaA	1.28	*umuD*	3.15	*yjbJ*	1.33	*flgL*	-4.7	*speE*	-1.26
hdeA	3.36	*wcaD*	1.58	*yjbM*	1.04	*flgM*	-4.73	*sufD*	-1.21
hdeB	3.14	*wcaE*	1.79	*yjbR*	1.46	*flgN*	-4.71	*tap*	-5.49
hdeD	2.74	*wcaF*	1.38	*yjeN*	1.48	*flhA*	-3.2	*tar*	-6.11
hflB	1.17	*xapR*	1.41	*yjfJ*	1.14	*flhB*	-3.99	*thrA*	-2.41
hha	1.14	*xisE*	5.66	*yjfK*	2.32	*flhE*	-3.66	*thrB*	-2.07
hlyE	1.28	*yacL*	1.51	*yjhI*	2.67	*fliA*	-5.4	*thrC*	-2.18
htrL	1.46	*yadC*	1.19	*ymfD*	1.9	*fliC*	-5.69	*trg*	-2.32
hybO	1.86	*yadI*	1.17	*ymfJ*	5.96	*fliD*	-5.47	*trpE*	-6.27
idnD	1.05	*yadK*	1.81	*ymfL*	4.8	*fliE*	-4.31	*tsr*	-4.83
intE	5.64	*yafK*	1.14	*ymfM*	4.33	*fliF*	-5.2	*tyrR*	-1.11
iraP	1.46	*yafQ*	1.24	*ymfN*	4.16	*fliG*	-5.35	*ves*	-2.74
lamB	2.47	*yagK*	1.1	*ymfQ*	3.33	*fliH*	-5.08	*ycgR*	-4.96

lit	1.59	*yagL*	1.14	*ymfR*	3.51	*fliI*	-5.15	*yciT*	-2.06
Gene	**log_2FC**	**Gene**	**log_2FC**	**Gene**	**log_2FC**	**Gene**	**log_2FC**	**Gene**	**log_2FC**
livJ	3.18	*yahA*	2.59	*ymfS*	1.16	*fliJ*	-5.38	*yciZ*	-1.71
lrhA	1.2	*yahL*	1.17	*ymfT*	4.37	*fliK*	-4.84	*ycjF*	-1.3
lysU	3.38	*ybaJ*	1.44	*ymgA*	4.91	*fliL*	-5.47	*ycjQ*	-1.12
malK	2.88	*ybaS*	1.58	*ymgB*	4.16	*fliM*	-5.51	*ycjU*	-1.5
malM	2.4	*ybaT*	1.29	*ymgC*	3.54	*fliN*	-4.99	*ycjX*	-1.23
malP	1.57	*ybbC*	2.21	*ynbB*	1.27	*fliO*	-4.86	*ydcA*	-1.11
malQ	1.14	*ybcL*	1.71	*yoaC*	1.37	*fliP*	-4.89	*ydcM*	-1.16
matA	2.14	*ybcM*	1.88	*yoeB*	1.78	*fliQ*	-4.66	*yddA*	-3.21
mcrA	2.16	*ybcS*	1.03	*ypfM*	2.56	*fliR*	-3.34	*yddB*	-3.09
mdtE	1.36	*ybeD*	1.31	*yrbL*	1.06	*fliS*	-5.18	*ydeA*	-1.41
mdtF	1.57	*ybhQ*	1.48	*zntR*	1.55	*fliT*	-4.95	*ydeE*	-1.24
mokC	1.31	*ybiU*	1.08	*aceA*	-2.42	*fliZ*	-5.22	*ydfH*	-1.21
mqsR	4.15	*ybiV*	1.03	*aceB*	-2.5	*flxA*	-4.8	*ydfX*	-1.12
nrdA	1.26	*ycbW*	2.27	*aceK*	-2.25	*gcvH*	-2.46	*ydfZ*	-1.82
nrdB	1.43	*ycdT*	2.72	*adk*	-1.27	*gcvP*	-2.41	*ydgA*	-1.04
obgE	1.93	*ycdU*	2.83	*aroA*	-1.19	*gcvT*	-2.74	*ydgI*	-1.03
osmB	1.62	*yceJ*	1.72	*aroH*	-2.63	*gltB*	-5	*ydiE*	-2.23
pabC	1.47	*yceO*	1.51	*bglX*	-1.06	*gltD*	-4.65	*yecR*	-2.7
phoA	1.57	*ycfK*	1.63	*carA*	-2.79	*hisA*	-1.03	*yeiE*	-1.14
potE	1.11	*ycgZ*	3.68	*carB*	-2.43	*hisH*	-1.09	*ygfF*	-1.97
proV	1.62	*ydhY*	1.04	*cheA*	-5.78	*hmp*	-1.25	*yghJ*	-1.27
pspG	1.7	*ydjF*	1.42	*cheB*	-5.11	*htpG*	-1.3	*yhhJ*	-1.24
purC	1.19	*ydjH*	1.1	*cheR*	-5.34	*ilvH*	-1.57	*yhjG*	-1.17
qseB	1.64	*yeaI*	1.29	*cheW*	-6.09	*ilvI*	-1.81	*yhjH*	-4.97
qseC	1.03	*yebF*	2.41	*cheY*	-5.37	*leuA*	-1.73	*yjcZ*	-3.12
rbsD	1.87	*yebG*	2	*cheZ*	-5.13	*leuB*	-1.98	*yjdA*	-1.44
rcsA	1.75	*yebN*	1.96	*cirA*	-2.34	*leuC*	-1.93	*ykfB*	-1.11
recA	2.35	*yedW*	1.23	*codA*	-1.7	*leuD*	-1.76	*ymdA*	-2.5

Table S2: Confirmation of fold change obtained from microarray with qPCR [related to Figure 1]: Mean log_2FC of 3 DEGs viz. *folA*, *hdeA* and *gadX* in 4xR1, 4xR2, 32xR1 and 32xR2 obtained from microarray and qPCR (*rplF* and 16s as housekeeping controls). The qPCR was carried out using the same RNA that was used for microarray.

Gene	Type	4xR1	4xR2	32xR1	32xR2
folA	Microarray	2.85	3.87	4.7	3.78
folA	rplF	3.49	3.64	5	3.45
folA	16s	3.01	3.86	4.32	3.63
hdeA	Microarray	2.51	3.71	3.82	3.02
hdeA	rplF	2.8	3.44	4.47	3.14
hdeA	16s	2.31	3.65	3.79	3.32
gadX	Microarray	2.23	1.98	3.51	3.27
gadX	rplF	2.6	1.61	3.36	2.92
gadX	16s	2.11	1.82	2.67	3.09

Table S3: Selection of top-ranked shortest paths (top-paths) for 32xTopNet generation [related to Figure 2]: Shortest paths were sorted according to path cost and subsets of top-ranked shortest paths (top-paths) were analysed. DEG enrichment was estimated for different subsets. The number provided in bracket is the percentage of total genes (G=3435) or DEGs (D=345) that were picked in a particular subset. For topnet extraction, we sought a subset such that $d > 0.75*D$ and hypergeometric enrichment p-value ≤ 0.05. The hypergeometric probability is a measure of how many successes (DEGs-d) are included in a subset of the population (topnet-g) as compared to successes (D) present in the entire population (G). Subset containing top 0.4% top-ranked shortest paths (top-paths) was seen to satisfy these requirements.

% Top-paths	No. of Paths	Total no. of genes (g) (%)	DEGs (d) (%)	Enrichment p-value
0.05	4207	511 (15)	117 (34)	3.27E-22
0.1	8413	923 (27)	157 (45)	2.96E-16
0.15	12621	1478 (43)	203 (59)	3.66E-11
0.2	16828	2040 (59)	235 (68)	4.61E-05
0.25	21035	2172 (63)	240 (70)	0.001
0.3	25242	2308 (67)	248 (72)	0.007
0.35	29449	2415 (70)	252 (73)	0.047
0.4	**33656**	**2509 (73)**	**269 (78)**	**0.003**
0.45	37863	2863 (83)	292 (85)	0.086
0.5	42070	2961(86)	296 (86)	0.345

Table S4: : Confirmation of upregulation of genes in 32xR *E. coli* with qPCR [related to Figure 2]: (a) Normalized fold expression of: *glyA*, *csgD*, GASR (*gadA*, *gadB*, *gadE*) genes in WT grown in 0.125 µg/mL TMP, and 32xR1, 32xR2 and the clinical isolate (CI) grown in absence of TMP (b) *gcvT* in WT grown in 0.125 µg/mL TMP and CI grown in 16 µg/mL TMP; as compared to WT grown in the absence of TMP. Average of two replicates is shown (c) Primers and annealing temperatures.

(a) Normalized fold expression

Gene	WT-0.125 µg/mL TMP	32xR1	32xR2	CI
glyA	2.24	28.24	1.08	1.86
csgD	0.90	32.45	0.43	32.77
gadA	2.01	11.41	13.96	33.10
gadB	2.78	6.74	7.66	45.57
gadE	3.09	1.41	9.49	85.09

(b) Normalized fold expression

Gene	WT-0.125 µg/mL TMP	CI-16 µg/mL TMP
folA	3.42	2.14
gcvT	0.29	0.69
glyA	3.12	2.00

(c) Primers and annealing temperatures

Gene	Primer sequence (5'-3')		T_A (°C)
16s rRNA	FP	CGGACGGGTGAGTAATGTCT	58
	RP	CTCAGACCAGCTAGGGATCG	
glyA	FP	GGCTGGACGTTAGCGTAGTC	58
	RP	CTGATCGCCTCCGAAAACTA	
csgD	FP	CGATGAGTAAGGAGGGCTGA	58
	RP	TACCGCGACATTGAAAACTG	
gadA	FP	TTATGGACGTTTTCGTCGTC	55
	RP	GAAGCTGTTAACGGATTTCC	
gadB	FP	GCGGATTGCGGATATTCTTC	55
	RP	AGAATCAAAACGTTTTCCGC	
gadE	FP	TGGTAAACACTTGCCCCATAA	55
	RP	GTGACGATGTCGCTCATACG	
gcvT	FP	TGCCTCTGGCGGTGTGATAG	58
	RP	ACAGTGTGGCAGCTTTTGCC	
folA	FP	GATTGCGGCGTTAGCGGTAG	58
	RP	TTACGCGATCGTCCGTACCC	

Table S5: Generations completed after a particular number of hours by BW25113 and its *glyA* knockout [related to Figure 3]: It is seen that both strains complete similar number of generations after every 12 hours. Over a period of 14 days, ~180 generations are completed.

Hours	BW25113: mean	BW25113: SD	Δ*glyA*: mean	Δ*glyA*: SD
Dec-24	6.24	0.03	6.43	0.13
36	12.92	0.14	13.26	0.13
48	19.53	0.37	20.8	0.03
60	26.28	0.11	26.8	0.11
72	32.88	0.14	33.41	0.08
84	39.15	0.21	39.53	0.3
96	45.57	0.17	45.96	0.1
108	52.52	0.13	53.12	0.12
120	59.34	0.13	59.79	0.25
132	65.87	0.07	66.2	0.22
144	72.39	0.15	72.91	0.48
156	79.06	0.14	79.25	0.56
168	85.8	0.17	85.75	0.57
180	92.38	0.1	93.13	0.17
192	99.03	0.13	99.66	0.18
204	105.28	0.1	105.97	0.15
216	112.63	0.1	112.94	0.29
228	119.17	0.91	119.36	0.8
240	125.57	0.1	126.2	0.14
252	132.63	0.13	132.67	0.28
264	139.1	0.07	139.43	0.21
276	145.69	0.13	146.21	0.23
288	152.27	9.25	152.91	0.14
300	159.08	0.09	159.47	0.25
312	165.62	0.22	166.41	0.13
324	172.09	0.12	172.79	0.08
336	178.11	0.16	179.3	0.24

Transparent Methods

Strains, media, antibiotics and growth conditions: *E. coli* K12 MG1655 was used as the WT parent for evolution of 32xR (TMP-resistant) *E. coli*. Another K12 strain- *E. coli* BW25113 and BW25113:Δ*glyA* from the Keio collection, used for comparative evolution were purchased from the Coli Genetic Stock Centre, Yale University, New Haven, USA and revived using LB and LB-25 µg/mL kanamycin respectively as per instructions (Baba et al., 2006). The MDR-clinical isolate of uropathogenic *E. coli* was obtained from Ramaiah Memorial Hospital, Bangalore, India. All strains were grown in M9 minimal medium supplemented with 0.4% glucose and 0.4% Bacto™ casamino acids, at 37ºC and 180 rpm. The clinical isolate and 32xR *E. coli* were maintained in M9-16 µg/mL TMP to prevent loss of resistance. TMP (2 mg/mL), kanamycin (50 mg/mL) and chloramphenicol (35 mg/mL) were prepared in DMSO, distilled water and methanol respectively, filter sterilized and stored at -20ºC.

Minimum inhibitory concentration (MIC) measurement: Two-fold serial dilutions of TMP were prepared in a sterile 96- well plate in a final volume of 100 µL per well and inoculated with an appropriately diluted overnight culture such that each well contained ~5 x 10^5 cells. Estimation of cell density was carried out using freshly prepared McFarland's turbidity standard no. 0.5 (0.05 mL 1% $BaCl_2$ and 9.95 mL 1% H_2SO_4). The lowest concentration that visibly inhibited growth (A_{600} < 0.2) was noted as the MIC. Experiments were performed in triplicates.

Evolution of TMP-resistant (32xR) *E. coli*: Two well isolated colonies were selected and overnight cultures of the same were used to inoculate (1%) 20 mL M9 for WT controls and M9 with a sub-inhibitory concentration of TMP (0.125 µg/mL; 0.25 x MIC) for the evolution of resistant *E. coli*. Thus, a control and a resistant culture were derived from each colony. The TMP exposed cultures were allowed to attain an A_{600} ~ 0.6, following which they were used to inoculate the next batch of media containing a two-fold higher concentration of TMP, such that the initial A_{600} was at least 0.1. In all iterations thereafter, the TMP concentration was doubled until a concentration of 16 µg/mL (32 x MIC) was achieved. Adaptation beyond this concentration was not continued since it is likely to be outside the physiologically encountered range, as TMP is toxic to the host at a concentration of 20 µg/mL (Schulz and Schmoldt, 2003).

Microarray and transcriptome analysis

Samples: Cells were harvested from 40 mL exponential phase (A_{600} ~ 0.5) cultures of WT1, WT2, 4xR1, 4xR2, 32xR1 and 32xR *E. coli* at 5000 rpm for 10 minutes, snap frozen and stored at -80ºC. RNA was extracted using RNeasy Mini Kit (Qiagen). Quantification and estimation of purity with $A_{260/280}$ was done using NanoDrop ND-1000 spectrophotometer (NanoDrop Technologies). Integrity of RNA was verified on Agilent 2100 Bioanalyzer using RNA 6000 Nano LabChip (Agilent Technologies).

Labelling and hybridization: Labelling was performed using Quick-Amp Labelling Kit, One Colour Part Number 5190-0442 (Agilent Technologies), which employs T7 RNA polymerase which simultaneously amplifies target RNA and incorporates Cy3-labelled CTP. Hybridization of labelled RNA was done using Gene Expression Hybridization Kit (Agilent Technologies). A custom *E. coli* 8x15k array (AMADID: 019439) was used. RNA extraction, hybridization and data collection were done by Genotypic Technology Private Limited, Bangalore, India.

Transcriptome analysis: Raw data was processed using the limma package of R Bioconductor (Gentleman et al., 2004; Ritchie et al., 2015). Pre-processing included background correction, quantile normalization and filtering out of control and low expressing probes (R code in Supplementary Files). To filter out low expressing probes, 95th percentile of intensity values of all negative control probes on the array was calculated and probes expressing at least 15% brighter than this value were retained. Normalized signal intensity values for genes were obtained as corrected $\log_2$ transformed, probe averaged values of their respective raw signal intensities. Data fitting was performed using the linear modelling function "lmFit" in the limma package and a pairwise comparison between gene expression profiles of the three conditions was carried out to identify differentially expressed genes (DEGs): genes with $\log_2$Fold Change (FC) ≥ 1 (FDR-adjusted p-value < 0.05) between the WT and 4xR or 32xR *E. coli* were considered as DEGs. Gene enrichment analysis for DEGs was carried out using PANTHERv13 and the ClueGo v2.3 (Bindea et al., 2009; Mi et al., 2010).

***E. coli* protein-protein interaction network (EcPPIN) and 32xNet construction:** Base network/EcPPIN: Interactions between proteins in *E. coli* MG1655 were downloaded from STRING database v10 (Szklarczyk et al., 2015). STRING is a collection of direct (physical) and indirect (functional/regulatory) interactions between proteins observed through experiments or predicted (inferred) from bioinformatics methods based on domain fusion, phylogeny, gene co-expression and gene neighbourhood considerations. Each interaction in the database is associated with a confidence score on a scale of 0 to 1000 and interactions with score ≥ 700 are marked as "high-confidence". Only 19750 high-confidence interactions with a combined score ≥ 850 or experimental score ≥ 700 were selected. Mapping of gene names to b numbers (STRING v10 uses b numbers) was done using EcoGene 3.0 database (Zhou and Rudd, 2013). Finally, 19022 interactions between 3435 proteins for which we had gene expression data were retained for further analysis.

Several biological interactions are unidirectional and therefore, adding directions to a protein interaction network makes it biologically meaningful. Directions for regulatory interactions (TF → gene) were obtained from STRING v10, RegulonDB v7, EcoCyc and a study on organization of gene regulation in *E. coli* (Gama-Castro et al., 2011; Keseler et al., 2011; Shen-Orr et al., 2002; Szklarczyk et al., 2015). Directions for metabolic interactions were obtained from the *E. coli* genome scale metabolic reconstruction model iJO1366 using code developed earlier for extracting directed interactions between enzymes from a mathematical model (Asgari et al., 2013; Orth et al., 2011). Directions for interactions between genes encoding two component

systems were obtained from the KEGG database (Kanehisa and Goto, 2000). After a final round of manual curation, a high-confidence genome scale network, EcPPIN, containing 3498 genes and 24542 interactions of which 13631 (55.5%) were directed, was obtained.

32xNet: For 32xNet construction, weights were added to the genes (nodes) in EcPPIN i.e. it was made condition-specific to reflect transcriptomic differences between WT and 32xR *E. coli*. The node weight (NW) for a gene i in EcPPIN was the absolute log_2FC calculated as;

$$NW_i = |R_i - W_i|$$

where R_i and W_i are the fitted mean log_2 transformed signal intensities of gene i in 32xR (mean of 32xR1 and 32xR2) and WT (mean of WT1 and WT2) respectively.

Edge weight (EW_{ij}) for an interaction between genes i and j was calculated as;

$$EW_{ij} = NW_i \times NW_j$$

Shortest paths estimation and analysis of 32xTopNet: Inversed edge weight(s) (EW'_{ij}) for implementation of Dijkstra's algorithm were calculated as;

$$EW'_{ij} = (EW_{max}+EW_{min}) - EW_{ij};$$

where EW_{max} and EW_{min} are the maximum and minimum edge weights in the network. Finally, normalized path cost was calculated as

$$\text{Path cost} = (\Sigma EW'_{ij})/n$$

where n is the number of edges in the path.

Shortest paths were sorted(ranked) according to path cost and subsets (0.05% to 0.5% paths at an interval of 0.05%) containing top-ranked shortest paths (top-paths) were evaluated for DEG enrichment with hypergeometric test using SuperExactTest considering a total (n) of 3435 genes (Wang et al., 2015) (Table S3). Identification of clusters was done using ClusterONE in Cytoscape (Nepusz et al., 2012; Shannon et al., 2003).

Biofilm quantification

Crystal violet staining: WT was grown in 2 mL M9, M9-0.125 mg/L TMP and M9-0.25 mg/L TMP and 32xR strains were grown in 2 mL M9 and M9-16 mg/L TMP over a period of 5 days at room temperature without shaking in 24-well plates. Post incubation, the culture was decanted, the wells were gently washed with PBS and stained with 1% crystal violet for 15 minutes. Excess unbound dye was rinsed away with three distilled water washes. Quantification of the biofilm on the sides and the bottom of each well was done by dissolving the crystal violet with 2 mL absolute ethanol and recording the absorbance spectrophotometrically at 590 nm.

Scanning electron microscopy: The experiment was set up as described for the crystal violet staining with the addition of a sterile coverslip at the bottom of each well. Post incubation, the

culture was decanted, and the coverslips were transferred to clean wells, fixed with 2.5% glutaraldehyde for 24 hours at 4 ºC and washed with PBS post incubation. Serial dehydration was carried out using pre-chilled 30%, 50%, 70%, 80%, 90%, 95% and 100% ethanol. Vacuum desiccated coverslips were coated with gold for 38 seconds and images at 4000X, 8000X and 12000X were recorded using Thermo Scientific™ Quanta™ ESEM™ microscope.

Generation of *glyA* knockouts: Gene knockout was performed according to the protocol described elsewhere (Datsenko and Wanner, 2000). Briefly, *E. coli* was transformed with a plasmid pKD46 which has the red recombinase enzyme under the control of PBAD promoter, inducible by arabinose. Transformants harbouring pKD46 were grown in 5 mL of M9 containing ampicillin (50 µg/mL) and L-arabinose (20 mM) at 30°C. pKD3 was used for the amplification of the chloramphenicol resistance gene. Competent cells were transformed with the chloramphenicol resistance gene flanked by the homologous sequence of *glyA*. Transformants were selected on chloramphenicol (35 µg/mL) containing M9 plate. Putative knockout colonies were screened by a PCR based method with confirmatory primers and chloramphenicol resistance internal primers. The sequences of the primers used in this study are: 5'CTGTTATCGCACAATGATTCGGTTATACTGTTCGCCGTTGCATATGAATATCCTCCTTAG3' (Forward) and 5'ACATTGACAGCAAATCACCGTTTCGCTTATGCGTAAACCGGTGTAGGCTGGAGCTGCTTC3' (Reverse).

Comparative evolution: In a 96 well plate, two-fold dilutions of TMP were prepared ranging from 16 µg/mL to 0.125 µg/mL in a final volume of 100 µL and inoculated with 1 µL log phase cultures of BW25113:Δ*glyA* and its wild-type parent *E. coli* BW25113 obtained from 6 well isolated colonies of each strain. The plate was incubated at 37 ºC for 12 hours and 1 µL culture from the well with the highest TMP concentration showing an $A_{600} \geq A_{600}$ of the corresponding well without TMP (un-inhibited growth), was used to inoculate the next plate. Successive inoculations were carried out every 12 hours for 14 days. The generations completed in 12 hours for each replicate were calculated using a previously used formula (Zampieri et al., 2017): $\log_2(A_{600}\ (fin)/A_{600}(0)/100)$; where $A_{600}(fin)$ is the A_{600} obtained after 12 hours for a well X and $A_{600}(0)$ is the A_{600} of the well from which 1 µL of the culture was taken for inoculation of well X.

Supplemental references

Asgari, Y., Salehzadeh-Yazdi, A., Schreiber, F., and Masoudi-Nejad, A. (2013). Controllability in cancer metabolic networks according to drug targets as driver nodes. PLoS ONE *8*, e79397.

Baba, T., Ara, T., Hasegawa, M., Takai, Y., Okumura, Y., Baba, M., Datsenko, K.A., Tomita, M., Wanner, B.L., and Mori, H. (2006). Construction of Escherichia coli K-12 in-frame, single-gene knockout mutants: the Keio collection. Mol. Syst. Biol. *2*, 2006.0008.

Bindea, G., Mlecnik, B., Hackl, H., Charoentong, P., Tosolini, M., Kirilovsky, A., Fridman, W.-H., Pagès, F., Trajanoski, Z., and Galon, J. (2009). ClueGO: a Cytoscape plug-in to decipher functionally grouped gene ontology and pathway annotation networks. Bioinformatics *25*, 1091–1093.

Datsenko, K.A., and Wanner, B.L. (2000). One-step inactivation of chromosomal genes in Escherichia coli K-12 using PCR products. Proc. Natl. Acad. Sci. U.S.A. *97*, 6640–6645.

Gama-Castro, S., Salgado, H., Peralta-Gil, M., Santos-Zavaleta, A., Muñiz-Rascado, L., Solano-Lira, H., Jimenez-Jacinto, V., Weiss, V., García-Sotelo, J.S., López-Fuentes, A., et al. (2011). RegulonDB version 7.0: transcriptional regulation of Escherichia coli K-12 integrated within genetic sensory response units (Gensor Units). Nucleic Acids Res. *39*, D98-105.

Gentleman, R.C., Carey, V.J., Bates, D.M., Bolstad, B., Dettling, M., Dudoit, S., Ellis, B., Gautier, L., Ge, Y., Gentry, J., et al. (2004). Bioconductor: open software development for computational biology and bioinformatics. Genome Biol. *5*, R80.

Kanehisa, M., and Goto, S. (2000). KEGG: kyoto encyclopedia of genes and genomes. Nucleic Acids Res. *28*, 27–30.

Keseler, I.M., Collado-Vides, J., Santos-Zavaleta, A., Peralta-Gil, M., Gama-Castro, S., Muñiz-Rascado, L., Bonavides-Martinez, C., Paley, S., Krummenacker, M., Altman, T., et al. (2011). EcoCyc: a comprehensive database of Escherichia coli biology. Nucleic Acids Res. *39*, D583-590.

Mi, H., Dong, Q., Muruganujan, A., Gaudet, P., Lewis, S., and Thomas, P.D. (2010). PANTHER version 7: improved phylogenetic trees, orthologs and collaboration with the Gene Ontology Consortium. Nucleic Acids Res. *38*, D204-210.

Nepusz, T., Yu, H., and Paccanaro, A. (2012). Detecting overlapping protein complexes in protein-protein interaction networks. Nat. Methods *9*, 471–472.

Orth, J.D., Conrad, T.M., Na, J., Lerman, J.A., Nam, H., Feist, A.M., and Palsson, B.Ø. (2011). A comprehensive genome-scale reconstruction of Escherichia coli metabolism--2011. Mol. Syst. Biol. *7*, 535.

Ritchie, M.E., Phipson, B., Wu, D., Hu, Y., Law, C.W., Shi, W., and Smyth, G.K. (2015). limma powers differential expression analyses for RNA-sequencing and microarray studies. Nucleic Acids Res. *43*, e47.

Schulz, M., and Schmoldt, A. (2003). Therapeutic and toxic blood concentrations of more than 800 drugs and other xenobiotics. Pharmazie *58*, 447–474.

Shannon, P., Markiel, A., Ozier, O., Baliga, N.S., Wang, J.T., Ramage, D., Amin, N., Schwikowski, B., and Ideker, T. (2003). Cytoscape: a software environment for integrated models of biomolecular interaction networks. Genome Res. *13*, 2498–2504.

Shen-Orr, S.S., Milo, R., Mangan, S., and Alon, U. (2002). Network motifs in the transcriptional regulation network of Escherichia coli. Nat. Genet. *31*, 64–68.

Szklarczyk, D., Franceschini, A., Wyder, S., Forslund, K., Heller, D., Huerta-Cepas, J., Simonovic, M., Roth, A., Santos, A., Tsafou, K.P., et al. (2015). STRING v10: protein-protein interaction networks, integrated over the tree of life. Nucleic Acids Res. *43*, D447-452.

Wang, M., Zhao, Y., and Zhang, B. (2015). Efficient Test and Visualization of Multi-Set Intersections. Sci Rep *5*, 16923.

Zampieri, M., Enke, T., Chubukov, V., Ricci, V., Piddock, L., and Sauer, U. (2017). Metabolic constraints on the evolution of antibiotic resistance. Mol. Syst. Biol. *13*, 917.

Zhou, J., and Rudd, K.E. (2013). EcoGene 3.0. Nucleic Acids Res. *41*, D613-624.